

# A Robotic, Compact and Extremely High Resolution Optical Spectrograph for a Close-in Super-Earth Survey

Jian Ge, Scott Powell, Bo Zhao, Frank Varosi, Bo Ma, Sirinrat Sithajan, Jian Liu, Rui Li, Nolan Grieves, Sidney Schofield, Louis Avner, Hali Jakeman, William A. Yoder, Jakob A. Gittelmacher & Michael A. Singer

Department of Astronomy, University of Florida

Matthew Muterspaugh, Michael Williamson & J. Edward Maxwell  
Center of Excellence in Information Systems, Tennessee State University  
Email: [jge@astro.ufl.edu](mailto:jge@astro.ufl.edu)

## Abstract

One of the most astonishing results from the HARPS and *Kepler* planet surveys is the recent discovery of *close-in super-Earths* orbiting more than half of FGKM dwarfs. This new population of exoplanets represents the most dominant class of planetary systems known to date, is totally unpredicted by the classical core-accretion disk planet formation model. High cadence and high precision Doppler spectroscopy is the key to characterize properties of this new population and constrain planet formation models.

A new *robotic, compact* high resolution optical spectrograph, called TOU (formerly called EXPERT-III), was commissioned at the Automatic Spectroscopic Telescope (AST) at Fairborn Observatory in Arizona in July 2013 and has produced a spectral resolution of about 100,000 and simultaneous wavelength coverage of 0.38-0.9  $\mu\text{m}$  with a 4kx4k back-illuminated Fairchild CCD detector. The instrument holds a very high vacuum of 1 micro torr and about 2 mK temperature stability over a month. The early on-sky RV measurements show that this instrument is approaching a Doppler precision of 1 m/s (rms) for bright reference stars (such as Tau Ceti) with 5 min exposures and better than 3 m/s (P-V, RMS~1 m/s) daily RV stability before calibration exposures are applied. A pilot survey of 20  $V < 9$  FGK dwarfs, including known super-Earth systems and known RV stable stars, is being launched and every star will be observed ~100 times over ~300 days time window between this summer and next spring, following up with a full survey of ~150  $V < 10$  FGKM dwarfs in 2015-2017.

**Key words:** Doppler, exoplanets, high cadence, survey, high spectral resolution, optical spectrograph, FGKM dwarfs and high precision

## 1. Introduction

One of the most astonishing results from the HARPS (High Accuracy Radial velocity Planet Searcher) and Keck HIRES ground-based Doppler planet surveys and the NASA *Kepler* space transit planet mission is the discovery of *close-in super-Earths*, with radii  $R \sim 1-4R_{\oplus}$  and orbital periods  $P < 100\text{d}$  (within Mercury's orbit in the solar system), orbiting more than half of FGKM dwarfs<sup>1-6</sup>. This new population of exoplanets, totally absent from our solar system, is surprisingly common and represents the most dominant class of planetary systems known to date. The existence of these newly detected close-in super-Earths has challenged the classical core accretion planet formation model which predict “deserts” of reduced planet occurrence with low-mass planets in the close-in orbits<sup>7,8</sup> where both Doppler and transit surveys discover a great

abundance of low mass planets. This indicates that different mechanisms may have contributed to forming these dominant close-in low mass planets. Several models have been proposed to explain this close-in low mass planet formation<sup>9</sup>. The most popular ones include *in situ* formation models<sup>10-12</sup> and inward, type 1 migration of a population of planetary embryos<sup>9,13</sup>. Although these new models can correctly predict several observed properties of close-in low mass planets (such as the mass distribution, small eccentricities and inclinations and occurrence of multiple planets), many key properties of this new planet population (such as planetary system architectures and bulk compositions and stellar mass relationship) remain to be studied with observations. High cadence and high RV precision measurements of nearby bright FGKM dwarfs offer a powerful way to detect and characterize a large number of low-mass planets in the near future. New results of low mass planet properties (such as mass, radii and orbital parameters) from these ground-based high precision RV surveys in combination with space-based planet transit observations through future NASA *TESS* mission can be used to differentiate between these planet models<sup>9,14,15</sup>.

High cadence and high RV precision measurements of nearby bright FGKM dwarfs, especially K and M dwarfs, would also offer a very sensitive tool to locate low-mass rocky planets in the habitable zones (HZs) around these stars. Over the past few years, great progress has been made in identifying a few dozen low-mass planet candidates in the HZs of their parent stars<sup>16-22</sup>. A few of them have been identified around nearby bright M and K dwarfs with HARPS<sup>16,17,21</sup>. Most of these candidates were identified around faint *Kepler* stars, which can be primarily used for statistical study of  $\eta_{\oplus}$ , the frequency of Earth-size planets in and near the HZ of solar-type and late type stars<sup>18,23,24,25</sup>. It is extremely challenging to follow up these *Kepler* habitable Earth-size planets with ground-based RV instruments due to the faintness of their host stars. On the other hand, bright low-mass stars (such as K and M dwarfs) are excellent targets for searching for habitable terrestrial planets. This is because these low-mass stars are less luminous than the Sun and their HZs are much closer to the host stars than that in the solar system. The shorter orbital period of planets in the HZ of low mass stars and lower host star mass allow for easier detections with ground-based RV surveys. For instance, a Doppler instrument with RV precision of 1 m/s is capable of detecting and characterizing habitable planets with masses between  $\sim 2$  to  $10 M_{\oplus}$  around nearby K and M dwarfs<sup>26</sup>. M dwarfs, consisting of about 70% of all the main-sequence stars in the Milky Way<sup>27</sup>, are excellent targets for searching for habitable terrestrial planets in the solar neighbor.

Motivated by investigating these close-in super-Earth populations around nearby FGKM dwarfs and searching for habitable super-Earths around nearby K and M dwarfs, we developed a compact, extremely high resolution optical spectrograph called TOU (formerly named EXPERT-III)<sup>26</sup> in 2010-2013 and commissioned it at the 2 meter Automatic Spectroscopic Telescope (AST) at Fairborn Observatory in Arizona in July 2013. We tested and improved this spectrograph in 2013 and early 2014 and are launching a pilot robotic, high cadence ( $\sim 100$  RV measurements over 1 year) and high precision ( $\sim 1-2$  m/s) RV survey of 20 nearby bright FGK dwarfs ( $V < 9$ ) this summer through next spring and will continue to monitor additional  $\sim 150$  FGKM dwarfs ( $V < 10$ ) during 2015-2017 with a goal to obtain a large homogeneous sample of close-in super-Earths by the end of the survey. Bright targets can greatly help reduce RV measurement errors with the TOU Doppler spectrograph and also increase the survey speed for high cadence observations of the reasonable size of survey targets to draw statistically significant

conclusions. This survey would greatly reduce uncertainties in measuring survey completeness compared to previous HARPS and Keck eta-Earth planet surveys because of their sparse observational cadence and also totally eliminate false positives associated with the *Kepler* planet candidates. It can provide important complementary information to the exploding new knowledge accumulated by previous planet surveys.

Below we summarize on-sky performance of the TOU spectrograph and also introduce some details about the planned survey.

## 2. TOU Spectrograph Description and Performance

The TOU design follows the HARPS design, such as optics, the white pupil configuration, extremely high spectral resolution, vacuum operation, temperature control and fiber mode scrambling, but with several design refinements to significantly reduce its volume (a factor of

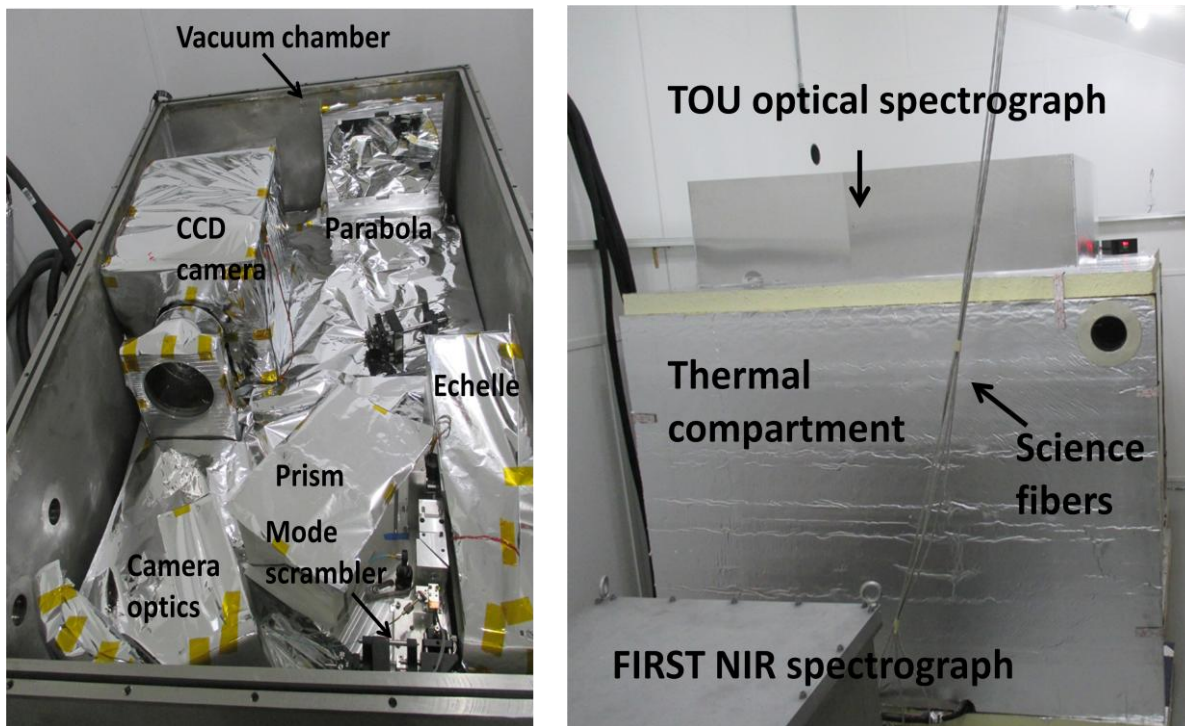


Figure 1. (Left). The inside of the TOU spectrograph. The spectrograph is bench-mounted inside a vacuum chamber. The spectrograph bench is 1.34 meter long and 0.8 meter wide. All the major instrument components and the bench are covered with 30 layer Multi-layer Insulation (MLI) to minimize their temperature variations caused by thermal radiation. (Right). The newly constructed thermal compartment to insulate the spectrograph from the A/C room to reduce its long-term temperature variations.

four) and construction cost (about \$1M), but substantially increase its wavelength coverage (a factor of 1.7 times) while maintaining its spectral resolution ( $R \sim 100K$ ) and instrument throughput. Design and operation parameters for TOU are summarized in previously published papers<sup>26,28</sup>. Figure 2.1 shows the inside of TOU, which is installed in a thermally controlled enclosure. The spectrograph system is inside an air-conditioned room with about temperature variation of 1-1.5°C (P-V) over a month. In order to further improve the instrument long-term thermal stability, a thermal compartment (Figure 2.1) was constructed and installed in early June

2014 to house the thermal enclosure and spectrograph. The temperature inside the compartment varies only about 0.1°C (Peak-to-Valley (PV)) over a week, which has further improved the instrument temperature stability (e.g., about 1 mK (rms) for the bench over a week).

The main difference between TOU and HARPS is the implementation of a 1 to 4 fiber coupling to slice one input 80 μm (2.1 arcsec on sky at the AST 2m) fiber beam into four 40 μm fiber beams and rearranged them in a row to reach a spectral resolution similar to HARPS (Figure 2.2) while halving the collimator beam diameter. This design change allows a factor of two reduction in optics size and instrument dimension, and a factor of four reduction in the instrument volume, while causing about 50% measured photon loss in the fiber coupling. We use two prisms as the cross-disperser with a measured efficiency of 96% for most of the wavelengths, instead of the grism cross-disperser in HARPS (an average transmission of 73%<sup>35</sup>). This design change has gained about 30% throughput, largely increased homogeneity of the spectral order separations, and produced nearly even spectral efficiency over the entire operation wavelengths. Operating the two prisms allows packing of an additional 22 spectral orders beyond 690 nm (690-900 nm) on a 4k×4k CCD detector (Figure 2.2) compared to HARPS, *resulting in a 1.7 times gain in the spectrograph wavelength coverage*. The extra gain at long wavelengths would greatly benefit RV measurements for late K and M dwarfs which have peak flux around 1000 nm<sup>29</sup>. The use of a 2.1 arcsec fiber would gain about 20-30% seeing coupling over the use of 1 arcsec fiber with HARPS under similar seeing condition. Therefore, the overall instrument throughput is comparable to HARPS.

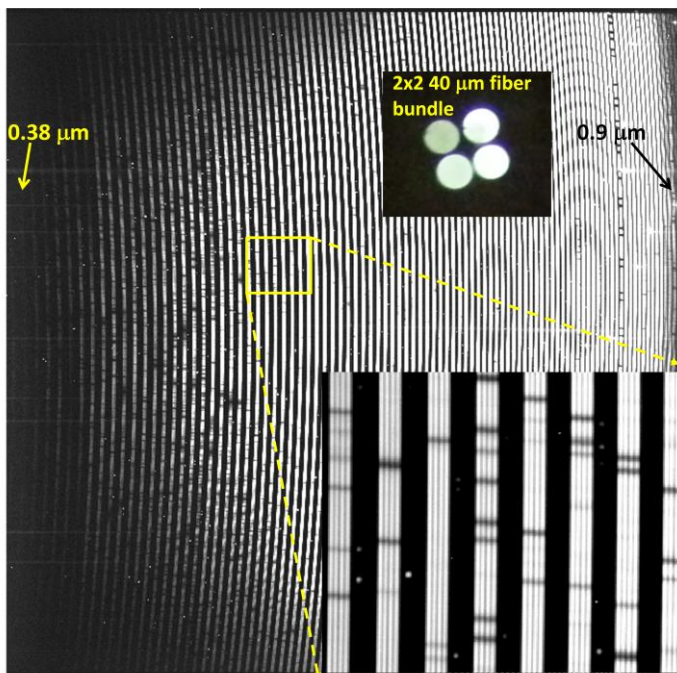


Figure 2.2. A stellar spectrum of Tau Ceti in 5 min exposure with the TOU EHR mode at R=100K. The ThAr calibration spectrum can be seen in the zoom-in spectrum. An image of a 2x2 fiber bundle is included, which rearranges the incoming 80 μm fiber beam into four 40 μm fiber beams on a row to double the spectral resolution.

### 2.1. TOU Measured Instrument Performance

TOU was commissioned at the AST 2m during the summer shutdown 2013. The instrument began its operation in late September with the ThAr calibration source to measure the instrument drift and calibration precision and was used to take on-sky data for several reference stars, such as Tau Ceti and 70 Vir, for testing on-sky RV measurement performance. Figure 2.2 shows Tau Ceti spectra taken with the TOU Extremely High Resolution (EHR) mode in 5 min exposures. The wavelengths from 380 nm to 900 nm are covered on the 4k×4k CCD, exactly matching the optical design. The smallest measured order separation is 25 pixels at 900nm. The average measured full width at half maximum (FWHM) of strong ThAr lines is about 3.3 pixels for EHR,

which is equivalent to a spectral resolution of  $R=100K$ . Figure 2.3 shows a part of reduced sky spectrum at the 561.5nm region and its comparison with the synthetic solar spectrum at  $R\sim 120K$  from the NSO solar spectrum template, indicating similar spectral resolution.

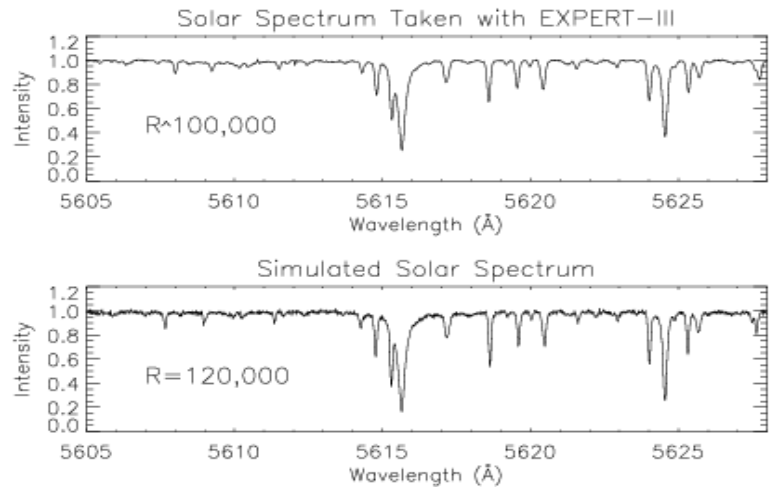


Figure 2.3. Reduced sky spectrum taken with the TOU  $R=100K$  mode (top) and comparison with a simulated solar spectrum at  $R=120K$ .

The measured overall detection efficiency (from above the atmosphere to the detector) at  $0.55 \mu\text{m}$  is 1.7% at the peak under a 2 arcsec seeing condition, a factor of 2.6 times lower than the forecast value under the 1.5 arcsec seeing condition (Figure 2.4). We have investigated causes for the additional photon losses and have identified a few sources such as atmospheric differential dispersion, the telescope's image aberration (large astigmatism) and the seeing loss (the typical seeing at Fairborn is about 2 arcsec). Efforts were made in early May 2014 to realign the telescope secondary and adjust the primary mirror mounts to reduce the image aberration. An atmospheric dispersion corrector (ADC) has been designed and will be manufactured late 2014 before installing it at the AST telescope. The implementation of the ADC alone would double the throughput at both blue and red wavelengths when observing a target at a high airmass (such as  $\text{secz}\sim 2$ ).

The instrument appears to be very stable. Our monitoring results show that the *instrument drifts less than 5m/s over 4 days (Figure 2.5)*. The RMS is  $0.0013\text{pixels}$  (or  $1.1 \text{ m/s}$ ), which is the same level as that achieved with *HARPS* over a month. Our analysis of ThAr spectra from the reference and the science beams show they are tracking each other within 1 m/s over 24 hours. Figure 2.5 also shows RV drifts for both beams and the residual after the science beam drift is subtracted with the reference beam drift. *The RMS of the residual is 0.00074 pixels, or 0.67 m/s, over 24 hours*, which is close to our survey requirement ( $\sim 0.4\text{m/s}$  calibration error). We added a temperature control in early May 2014 to input air to the cryotiger compressor and have reduced the temperature

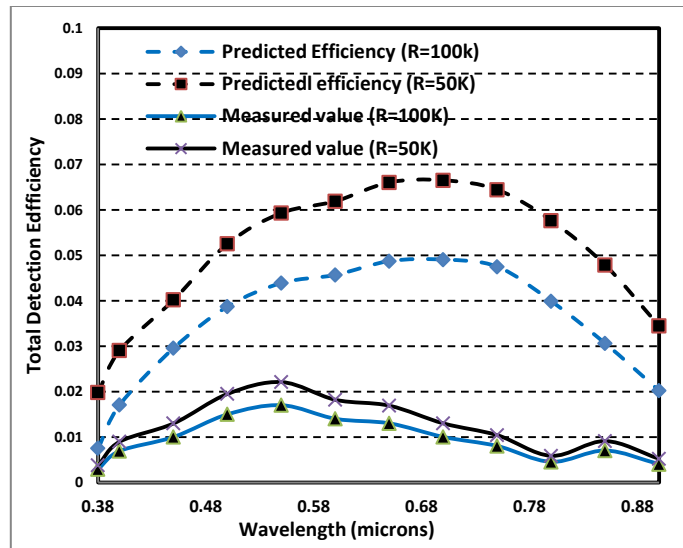


Figure 2.4. TOU overall detection efficiency from above the atmosphere to the detector (measured and predicted values) for both EHR and HR modes.

variation of the cryotiger lines (both supply and return lines) by a factor of three (from a P-V of  $\sim 0.5^\circ\text{C}$  to  $\sim 0.15^\circ\text{C}$ ). We implemented a temperature controlled compartment to house the entire TOU thermal enclosure and have further reduced the daily temperature variation of the instrument room caused by the diurnal temperature variation from current P-V of  $\sim 1^\circ\text{C}$  to

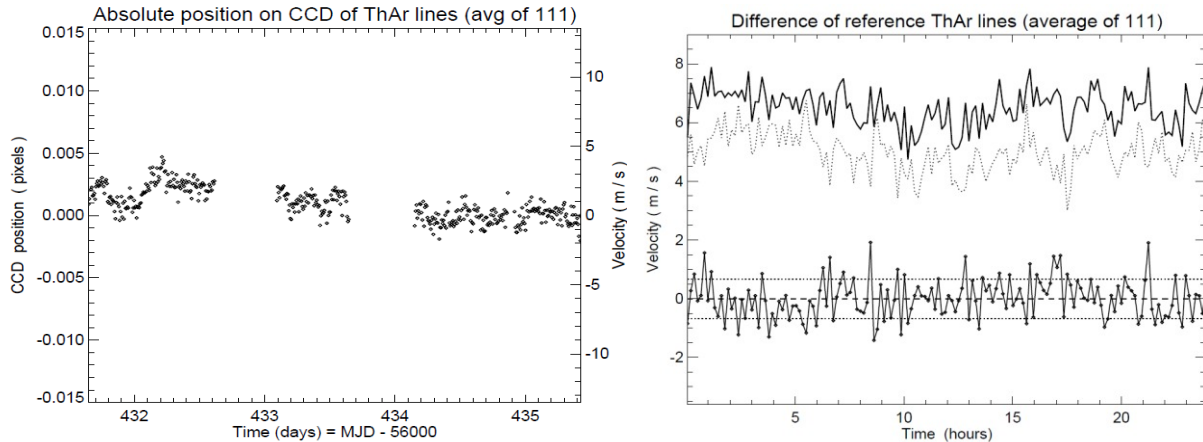


Figure 2.5. (Left). RV drifts with TOU over 4 days. (Right). RV drifts of the science beam (dashed line) and the reference beam (thin solid line) at the top. The bottom solid line show the rms of the residual (0.00074 pixels, corresponding to 0.67 m/s) after the science beam drift is subtracted.

$\sim 0.1^\circ\text{C}$ . Our goal is to reach a long term stability of about 1 m/s (RMS, or a P-V of about 4 m/s) over a month or longer. This improvement is likely to lead to a better RV calibration accuracy and reliability over a long term.

## 2.2. Measured Doppler Sensitivity and Stellar Jitters

Figure 2.6 shows the RV measurements for Tau Ceti. The RMS = 1.3 m/s over 16 days and the average photon noise limiting error  $\approx 0.25$  m/s. Our RMS error is slightly larger than that (0.92 m/s) reported by the HARPS measurements<sup>17</sup>. Both HARPS and our RV measurements of Tau Ceti suggest that the measurement error is likely dominated by stellar noises. Figure 2.6 also shows RV measurements of 70 Vir, a known giant planetary system<sup>30,31</sup>. The RMS of the residual is 3.4 m/s after the planet signal is subtracted while a reported RMS is 7.4 m/s in the literature. The relatively large RMS compared to the average photon-limited error (0.7 m/s in 5 min exposures) suggests that stellar noise may contribute to the RV uncertainties in this system. Our current data pipeline is still in the early development phase. We can only process the middle part of the spectral data (4972-6227 Å, or 26 spectral orders) and are improving our data pipeline capability in handling more spectral orders to hopefully achieve better RV measurement precision by combining RV measurements from more spectral orders.

Our RV measurements of stable stars have already demonstrated that stellar noises appear to contribute significantly to measurement uncertainties in our two reference stars (Tau Ceti and 70 Vir). RV measurements of two other reference stars, HD 109358 ( $V=4.3$ , G0V), HD 185144 ( $V=4.7$ , G9V), also indicate stellar noises probably dominate the measurement errors in the data. For instance, RMS = 1.9 m/s (photon error  $\approx 0.8$  m/s) and 2.3 m/s (photon error  $\approx 1.2$  m/s) over 10 days for HD 185144 and HD 109358, respectively. Our RMS errors are comparable to reported values, e.g., RMS=2.5 m/s for HD 185144 with Keck HIRES<sup>32</sup>, RMS=2.0 m/s for HD 109358 with SOPHIE+<sup>33</sup>. Therefore, mitigation of activity induced jitters in stellar RV measurements

becomes a critical part of our survey plan and strategy. Our survey targets will be vetted for their activity jitters and only those stars with stellar jitters less than 1.5 m/s will be chosen for the survey.

Due to the existence of stellar RV jitters (at the level of  $\sim 1.5$  m/s or better for some targets) in our final survey targets, an exposure time for a target needs to be just long enough to reach a negligible level of photon-limited noise compared to the stellar jitter. However, for those very bright stars ( $V < 6$ ), we still hold our exposure time to 10-15 min to average out RV noises caused

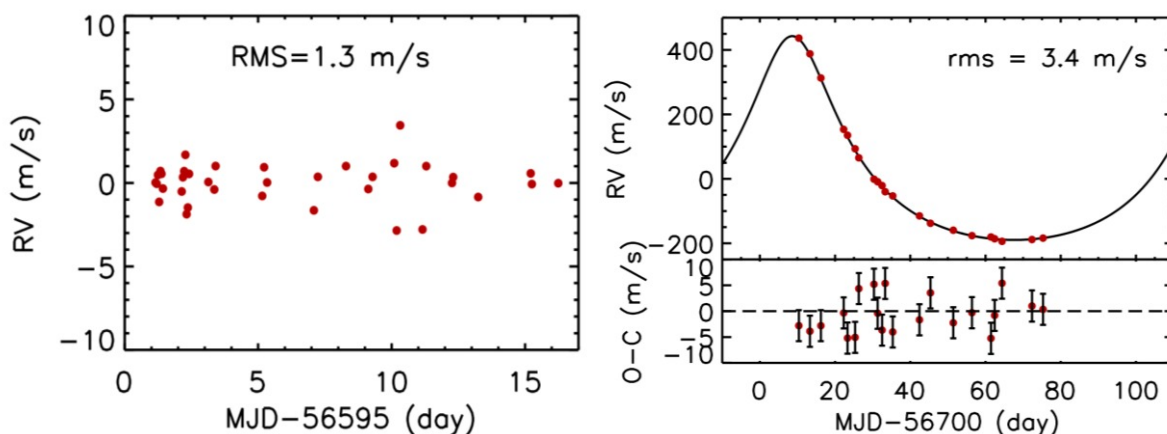


Figure 2.6. (Left). RV measurements of Tau Ceti over 16 days. rms = 1.3 m/s for 26 processed spectral orders (4972-6227Å), averaged with 9 measurements, and the average photon-limited error is 0.25m/s. (Right). RV measurements of 70 Vir over  $\sim 60$  days. The red dots are the measurements and the black line is the fit from the published curve. The RMS residual after removing the fit is 3.4m/s. The average photon error is 0.7m/s in 5 min exposures.

by stellar oscillations<sup>34</sup>. Besides the stellar jitters and photon errors, the real RV measurement errors include additional errors, such as uncertainties from instrument RV calibration, fiber illumination variations caused by the telescope guiding, tracking and seeing, instrument thermal drift and data processing. Table 2.1 summarizes the error budget in RV measurements of a typical survey star with slow rotational velocity (2 km/s). If we can keep these additional errors small ( $< 0.5$  m/s) and choose a target with stellar jitter well below 1 m/s, we can reach sub m/s precision. Otherwise; our RV measurements are likely limited by stellar noises. Based on our error considerations, optimistic and pessimistic cases of the RV performance are used in our performance simulations and planet yield forecasting summarized in the next section.

TOU was designed to keep those additional noises low<sup>26</sup>. For instance, we used two ThAr calibration sources (one as an operational one and the other as a master following HARPS calibration protocol<sup>35</sup>) to keep our calibration error to  $\sim 0.4$  m/s. The three-lenses optical fiber mode scrambler in TOU can control the illumination change, caused by the seeing or guiding, to within 0.3% (measured value), leading to the measurement error within 0.3 m/s. By controlling the

Table 2.1. Error budget for a K5V star with  $V_{\text{sin}i} = 2$  km/s,  $S/N = 100$  per pixel at  $0.55 \mu\text{m}$ .

Error source/mode	EHR
Photon	0.32 m/s
Calibration (ThAr)	$\sim 0.4$ m/s
Telluric absorption removal (2%)	$\sim 0.3$ m/s
Fiber illumination (guiding error)	$< 0.3$ m/s
Thermal differential drift	$< 0.3$ m/s
Data pipeline	$\sim 0.35$ m/s
Stellar jitter	$< 1.5$ m/s
<b>Total error w/o jitter</b>	$\sim 0.8$ m/s
<b>Total error w jitter</b>	$< 1.7$ m/s

instrument long-term thermal stability to peak-to-valley less than 2 mK, we can limit the differential drift between the calibration and science beams to within 0.3 m/s. The big uncertain area is the error caused by the data pipeline. Major efforts have been made and will continue to be made to extend our wavelength coverage for data processing and refine our data pipeline by correcting all of the instrument effects which contribute to notable RV uncertainties (such as the spectral slant, cosmic rays, scattered light and PSFs). Our goal is to keep the overall error caused by data processing comparable to the photon noise or less. This would allow us to reach 1-2 m/s RV measurement errors for most of the survey targets. The overall 1-2 m/s RV measurement uncertainties would allow us to seriously probe the close-in super-Earth population around FGKM dwarfs and also habitable super-Earths around K and M dwarfs<sup>26</sup>.

### 3. The High Cadence and High Precision Close-in Super-Earth Survey

Our TOU close-in super-Earth survey adopts a totally different planet survey strategy than previous low mass planet surveys using ground-based optical high resolution spectrographs<sup>36,1,21</sup>. Instead of surveying over a large number of targets with various measurements (from a few RV data points to ~400 RV data points for observing Alpha Cen B<sup>37</sup>), the TOU survey will offer a homogeneous high cadence for every survey target, i.e., 100 RV measurements randomly spread over ~300 days. We plan to monitor ~55 new targets each year. *The robotic (automatic) nature of the survey telescope at Fairborn Observatory and its flexible queue observation schedule are the key to realizing this homogenous high cadence.* This homogeneous high cadence will minimize the time aliasing in detecting low mass planets, especially those in highly eccentric

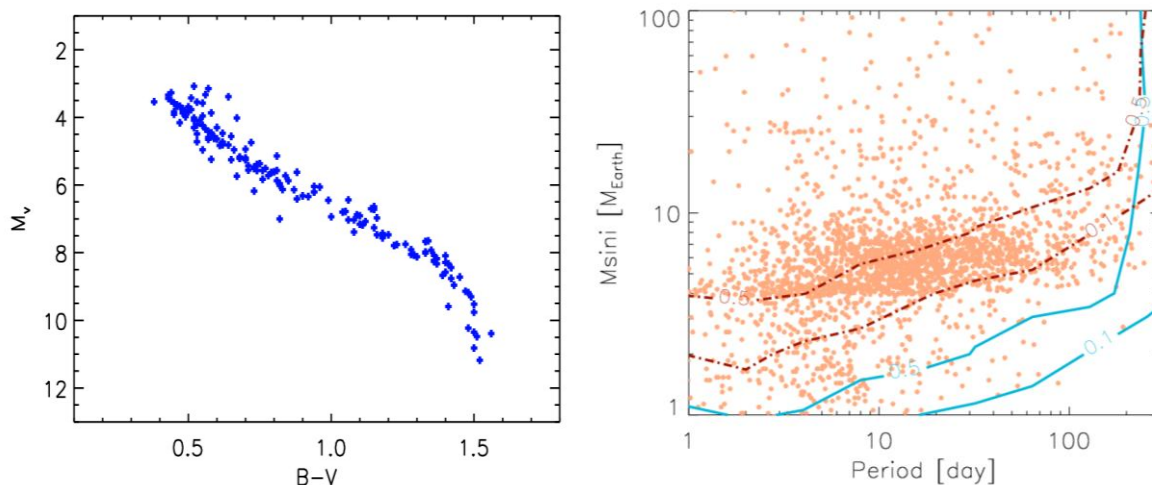


Figure 3.1. (Left). Absolute magnitude vs color distribution of our close-in low mass planet survey targets covering from F5V to M3.5V. (Right) The predicted contours (10% and 50%) of the TOU survey completeness (the blue and red lines represent the optimistic and the pessimistic cases) based on the survey targets, observation strategy, cadence and RV precision. Orange dots are Kepler planet candidates<sup>4</sup>. Masses of *Kepler* planet candidates are derived from the mass-radius relations<sup>14</sup>.

orbits, which tend to be largely missed in the previous surveys and *both detections and non-detections from the survey can be reliably used for statistical studies.* Thus, the proposed survey strategy, cadence and schedule will offer the best accuracy to assess the survey completeness. As illustrated in Figure 3.1, our survey strategy allows for probing most of the parameter space in the planet mass-period distribution of nearby bright low mass stars to independently verify characteristics (such as distribution and occurrence rates) of the close-in low mass planet

population identified by the *Kepler* mission. *This survey will offer the best homogeneous data set for constraining formation models of close-in low mass planets.* Moreover, it offers an unbiased sampling of HZs to assess habitability of close-in low mass planets around nearby K and M dwarfs.

### 3.1. Survey Target Selection

Our survey targets were selected from the following catalogs: Gliese Catalog of Nearby Stars (Spring 1989); Gliese Catalog of Nearby Stars cross identified with 2MASS<sup>38</sup>; ROSAT All-Sky Survey: Nearby Stars<sup>39</sup>. The selection was based on the following criteria:

- 1)  $V < 9.5$  and  $\text{DEC} > -20^\circ$
- 2)  $M_V < 11.2$  (corresponding to M3.5V)
- 3) Stellar activity,  $\log(R'_{\text{HK}}) < -4.8$ , for FGK dwarfs, or ratio between X-ray luminosity and bolometric luminosity,  $R_X < -3.0$ , if activity level is unknown
- 4) Number of targets are nearly equally distributed between 0.2-1.2 solar masses
- 5) No binary companion within 5 arcsec of the survey target

These criteria allow us to choose an unbiased survey sample with inactive stars and nearly equal mass distribution to maximize its sensitivity to probe low mass planet characteristics among FGKM dwarfs over the wide mass range.

Based on the empirical equation of rotation velocity vs.  $R_X$ <sup>40</sup>, we expect most of the  $R_X$  selected targets to have rotational velocity less than 5 km/s. Therefore, most of them are inactive stars, which can help our final survey target vetting process. Figure 3.2 shows the number distribution in the V band, the effective temperature distribution, and the stellar mass distribution of the survey targets. We have a total of 21 stars with less than 0.5 solar masses (M0-M3.5V).

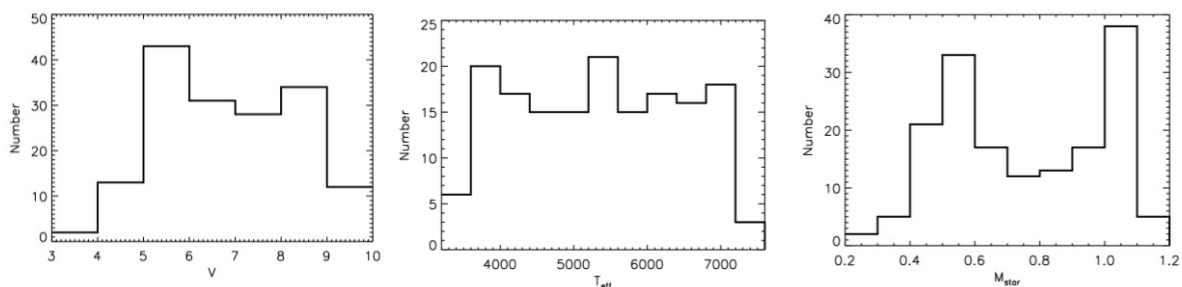


Figure 3.2. (Left). V magnitude distribution of selected stars for the TOU close-in super-Earth survey. (Middle).  $T_{\text{eff}}$  distribution of the selected survey targets. (Right). Stellar mass distribution of the selected survey targets.

### 3.2. Predicted Planet Yield

We conducted survey simulations to derive survey sensitivity and completeness. We adopted the planned cadence, schedule (100 RV measurements randomly distributed over 300 days) and real observation conditions (night time window and also average weather conditions at Fairborn Observatory) in the simulations. Two RV performance of the survey instrument are used in the simulations. One is based on RV measurement uncertainties from a combination of 1.5 times photon noise (including the pipeline error), calibration (0.5 m/s) and 2% telluric line removal error ( $\sim 0.3$  m/s) while the other includes an additional 2.0 m/s long term systematic error applied to all survey targets. The first consideration, representing possible RV performance for a survey star without significant activity induced RV jitters, is our optimistic case, while the

second consideration represents a possible pessimistic case in which survey stars have about an average level of activity induced RV jitters<sup>41</sup>. We will minimize the impact of stellar jitters on our RV performance by carefully selecting survey targets with unknown jitter levels through a reconnaissance pilot survey of those targets and reject those with jitter level above 1.5 m/s. In other words, our final survey targets would have jitter level less than 1.5m/s. Figure 3.1 shows survey detection sensitivity and completeness level from both optimistic and pessimistic cases. It is quite interesting to see that our proposed high cadence survey can detect nearly all of the known low-mass planet candidates identified by *Kepler* if we can reach high RV precision (~1m/s) for the majority of our survey targets. Even under the pessimistic case, we can still detect a majority (~80%) of the *Kepler* super-Earth population thanks to our high cadence strategy.

The predicted planet yields from both the optimistic and pessimistic cases are listed in Table 3.1. Our final yield is likely to fall between. We adopted the following planet occurrence rate within 300 days: Earth-size planets (1-1.25R<sub>⊕</sub>), 16.1%; super-Earths (1.25-2 R<sub>⊕</sub>), 32.9%; and small Neptunes (2-4 R<sub>⊕</sub>), 30.9%<sup>5</sup>. The mass for each planet is determined by empirical formula (equations (1), (2) and (3)) in Weiss & Marcy<sup>14</sup>. We used the planet occurrence rates for 0.8-245 days as our rates for the above calculations. For those which do not have the rates in this period range, we extrapolated the rates from those derived from the smaller period ranges (such as super-Earths and Earths) in Table 3 of Fressin et al's paper<sup>5</sup>. The large systematic measurement errors of 2 m/s applied to all of

the survey stars in the pessimistic case has a major effect on the detection sensitivity for Earth-size planets

and also super-Earths while it does not significantly affect the detection of close-in small Neptunes. About half of the super-Earths around K and M dwarfs in the optimistic and pessimistic cases, respectively) will be in their HZs (33% without cloud coverage and 73% with full cloud coverage) and one of them may be a transiting planet. Our optimistic detections would possibly provide sensitive measurements of planet occurrence rates for these three types of low mass planets. *This sample would also offer a large collection of HZ rocky planets around nearby K and M dwarfs using ground-based telescopes.* Our pessimistic detections would possibly offer sensitive measurements of planet occurrence rates for super-Earths and small Neptunes. In either case, the overall planet sample will substantially increase the power for statistical study of planet occurrence and properties and constraints on planet formation models and physical conditions around 0.2-1.2 solar mass stars.

Table 3.1. Predicted planet yields from the high cadence survey

	Earth-size	Super-Earths	Small Neptunes
Optimistic	10	36	39
Pessimistic	1	11	25

#### 4. Conclusions and Future Work

The TOU spectrograph has produced science quality data at the AST 2m automatic telescope. The overall measured instrument performance meets the design requirements except the overall detection efficiency (from above the atmosphere to the detector). Efforts have been made to improve the overall detection efficiency by improving the telescope image quality and are being made to implement an ADC and a better quality optical fiber (reducing its focal ratio degradation). Nevertheless, current instrument detection efficiency is sufficient to carry out the pilot survey, which targets FGK dwarfs with V<9, and reach the survey required Doppler sensitivity (~1-2 m/s) within 10-60 min exposures (1 hour exposures for V~8-9 K dwarfs). The

data pipeline is being improved to handle spectra between 0.38-0.7  $\mu\text{m}$ . A new generation calibration source, the Sine source, has been developed and demonstrated a factor of 3 times better calibration precision than the ThAr lamp<sup>42</sup>. This source, once ready for use, will improve RV calibration precision at 0.38-0.7  $\mu\text{m}$ . In addition, this Sine source can extend RV calibration coverage to 0.7-0.9  $\mu\text{m}$  where ThAr lamps have many saturated lines to ruin stellar spectrum quality for high precision RV measurements. This wavelength region is especially important for observing K and M dwarfs which have far more flux in this region than the bluer wavelengths.

**Acknowledgement:** This work has been supported by Dharma Endowment Foundation, DoD Cooperative Agreement W911NF-09-2-0017, the W.M. Keck Foundation, NSF-PAARE grant 1059158, state of Tennessee through its Centers of Excellence program and the University of Florida.

## REFERENCES

1. Mayor, M. et al. "The HARPS search for southern extra-solar planets XXXIV. Occurrence, mass distribution and orbital properties of super-Earths and Neptune-mass planets," *AsXiv*: 1109.2297v1 (2011).
2. Howard, A. et al., "Planet Occurrence within 0.25 AU of Solar-type Stars from Kepler," 201, 15 (2012).
3. Figueira, P. et al. "Comparing HARPS and Kepler surveys. The alignment of multiple-planet systems," *A&A*, 541, 139 (2012).
4. Batalha, N. et al. "Planetary Candidates Observed by Kepler. III. Analysis of the First 16 Months of Data," *ApJS*, 204, 24 (2013).
5. Fressin, F. et al. "The False Positive Rate of Kepler and the Occurrence of Planets," *ApJ*, 766, 81(2013).
6. Burke, C.J., et al. "Planetary Candidates Observed by Kepler IV: Planet Sample from Q1-Q8 (22 Months)," *arXiv*:1312.53581v1 (2014).
7. Ida, A. & Lin, D. "Toward a Deterministic Model of Planetary Formation. V. Accumulation Near the Ice Line and Super-Earths," *ApJ*, 685, 584 (2008).
8. Mordasini, C. et al. "Extrasolar planet population synthesis. I. Method, formation tracks, and mass-distance distribution," *A&A*, 501, 1139 (2009).
9. Raymond, S., Barnes, R., & Mandel, A. "Observable consequences of planet formation models in systems with close-in terrestrial planets," *MNRAS*, 384, 663(2008).
10. Hansen, B. & Murray, N. "Migration Then Assembly: Formation of Neptune-mass Planets inside 1 AU," *ApJ*, 751, 158 (2012).
11. Hansen, B. & Murray, N. "Testing in Situ Assembly with the Kepler Planet Candidate Sample," *ApJ*, 775, 53 (2013).
12. Chiang, E. & Laughlin, G. "The minimum-mass extrasolar nebula: in situ formation of close-in super-Earths," *MNRAS* 431, 3444 (2013).
13. Cossou, C., Raymond, S.N., & Pierens, A. "Convergence zones for Type I migration: an inward shift for multiple planet systems," *A&A*, 553, L2 (2013).
14. Weiss, L., & Marcy, G. W., "The Mass-Radius Relation for 65 Exoplanets Smaller than 4 Earth Radii," *ApJ*, 783, 6 (2014).
15. Marcy, G. et al. "Occurrence and core-envelope structure of 1--4x Earth-size planets around Sun-like stars," *ApJS*, in press (*arXiv*:1401.4195v1) (2014).
16. Udry, S., et al. "The HARPS search for southern extra-solar planets. XI. Super-Earths (5 and 8  $M_{\oplus}$ ) in a 3-planet system," *A&A*, 469, 43 (2007).
17. Pepe, F. et al. "The HARPS search for Earth-like planets in the habitable zone. I. Very low-mass planets around HD 20794, HD 85512, and HD 192310," *A&A*, 534, 58 (2011).
18. Borucki, W. et al. "Characteristics of Planetary Candidates Observed by Kepler. II. Analysis of the

- First Four Months of Data," *ApJ*, 736, 19 (2011).
19. Borucki, W. et al. "Kepler-22b: A 2.4 Earth-radius Planet in the Habitable Zone of a Sun-like Star," *ApJ*, 745, 120 (2012).
  20. Borucki, W. et al. "Kepler-62: A Five-Planet System with Planets of 1.4 and 1.6 Earth Radii in the Habitable Zone," *Sci.*, 340, 587 (2013).
  21. Bonfils, X. et al. "The HARPS search for southern extra-solar planets. XXXI. The M-dwarf sample," 549, 109 (2013).
  22. Quintana, E.V., et al. "An Earth-Sized Planet in the Habitable Zone of a Cool Star," *Sci.*, 344, 277 (2014).
  23. Kopparapu, R.K., "Habitable Zones around Main-sequence Stars: New Estimates," *ApJ*, 765, 131 (2013)
  24. Dressing, C.D., & Charbonneau, D. "The Occurrence Rate of Small Planets around Small Stars," *ApJ*, 767, 95 (2013)
  25. Gaidos, E. "Candidate Planets in the Habitable Zones of Kepler Stars," *ApJ*, 770, 90 (2013)
  26. Ge, J. et al. "Design and Performance of a New Generation, Compact, Low Cost, Very High Doppler Precision and Resolution Optical Spectrograph," *Proc. SPIE*, 8446E, 8RG (2012a).
  27. Kroupa, P., Tou, C.A., & Gilmore, G. "The distribution of low-mass stars in the Galactic disc," *MNRAS*, 262, 545 (1993).
  28. Zhao, B. & Ge, J. "Optical design of new generation compact, high resolution and high Doppler precision optical spectrograph," *Proc. SPIE*, 8446E, 84Z (2012).
  29. Leggett, S.K. et al. "Infrared Spectra of Low-Mass Stars: Toward a Temperature Scale for Red Dwarfs," *ApJS*, 104, 117 (1996).
  30. Butler, R.P., et al. "Catalog of Nearby Exoplanets," *ApJ*, 646, 505 (2006).
  31. Marcy, G., & Butler, R.P., "A Planetary Companion to 70 Virginis," *ApJ*, 464, 147 (1996).
  32. Wright, J. 2008, "The Jupiter Twin HD 154345b," *ApJ*, 683, 63 (2008).
  33. Bouchy, F., et al. "SOPHIE+: First results of an octagonal-section fiber for high-precision radial velocity measurements", 549, 49 (2013).
  34. Mayor, M. et al. "Setting New Standards with HARPS," *Messenger*, 20, 114 (2003).
  35. Pepe, F., et al. "HARPS: ESO's coming planet searcher. Chasing exoplanets with the La Silla 3.6-m telescope," *The Messenger* (ISSN 0722-6691), No. 110, p. 9 – 14 (2002).
  36. Howard, A. et al. "The Occurrence and Mass Distribution of Close-in Super-Earths, Neptunes, and Jupiters," *Science*, 330, 653 (2010).
  37. Dumusque, X. et al.. "An Earth-mass planet orbiting alpha Centauri B," *Nature*, 491, 207 (2012).
  38. Stauffer, J. et al. "Accurate Coordinates and 2MASS Cross Identifications for (Almost) All Gliese Catalog Star," *PASP*, 122, 885 (2010).
  39. Hunsch, M. et al. "The ROSAT all-sky survey catalogue of the nearby stars," *A&AS*, 135, 319 (1999).
  40. Kiraga, M., & Stepien, K. "Age-Rotation-Activity Relations for M Dwarf Stars," *AcA*, 57, 149 (2007).
  41. Wright, J. "Radial Velocity Jitter in Stars from the California and Carnegie Planet Search at Keck Observatory," *PASP*, 117, 657 (2005)
  42. Ge, J. et al. "On-sky Calibration Performance of a Monolithic Michelson Interferometer filtered source," *Proc. SPIE*, 7146, 8 (2014).